

Hydrological and seasonal controls of phosphorus in Northern Great Plains agricultural streams

Nora J. Casson¹, Henry F. Wilson², Stephanie Higgins¹

¹Department of Geography, University of Winnipeg, 515 Portage Ave. Winnipeg MB R3B 2E9

²Agriculture and Agri-Food Canada, Science and Technology Branch, Brandon Research and Development Centre, Brandon, MB, R7A 5Y3

Core Ideas

- Coherent seasonal patterns in stream phosphorus point to regional drivers
- Discharge is not the primary driver of total phosphorus dynamics in Prairie streams
- Stream phosphorus concentrations peak with snowmelt and in mid-summer
- Coherence with conductivity and temperature suggest drivers vary by season

1 **Abstract**

2 Controls on nutrient transport in cold, low relief agricultural regions vary dramatically among
3 seasons. The spring snowmelt is often the dominant runoff and nutrient loading event of the year.
4 However, climate change may increase the proportion of runoff occurring with rainfall and there
5 is an urgent need to understand seasonal controls on nutrient transport in order to understand
6 how patterns may change in the future. In this study, we assess patterns and drivers of total
7 phosphorus (TP) dynamics in eight streams draining agriculturally-dominated watersheds,
8 located in southern Manitoba, Canada. Data from three years of monitoring revealed highly
9 coherent patterns of TP concentrations in streams, with pronounced peaks in the spring and mid-
10 summer across the region. This coherent pattern was in spite of considerable interannual
11 variability in the magnitude and timing of discharge; in particular, a major storm event occurred
12 in summer 2014, which resulted in more discharge than the preceding spring melt.
13 Concentration-discharge model fits were generally poor or not significant, suggesting that runoff
14 generation is not the primary driver of TP dynamics in the majority of streams. Seasonal patterns
15 of conductivity and stream temperature suggest mechanisms controlling TP vary by season; a
16 spring TP concentration maximum may be related to surface runoff over frozen soils while the
17 summer TP maximum may be related to temperature-driven biogeochemical processes, which
18 are not well-represented in current conceptual or predictive models. These findings suggest that
19 controls on stream TP concentrations are dynamic through the year, and responses to increases in
20 dormant and non-dormant season temperatures may depend on seasonally-variable processes.

21 **1.0 Introduction**

22 Phosphorus (P) is a limiting nutrient in agricultural systems as well as freshwater ecosystems
23 (McCullough et al., 2012; Schindler, 2012). Excess P increases algae blooms and stimulates

24 plant growth, which increases respiration and decomposition which consumes oxygen and
25 creates anoxic environments (eutrophication) (Schindler et al., 2012). Transport of P from
26 watersheds to surface waters is promoted by human activities including agricultural practices
27 such as fertilizer use, irrigation, wetland drainage, land conversion, and soil erosion (Carpenter et
28 al., 1998; Bennett et al., 2012). Spatial patterns of soil P can vary considerably across
29 landscapes, and depend on factors such as management practices and landform (Wilson et al.,
30 2016). Wetlands generally act as long-term P sinks on the landscape, however P retention varies
31 depending on soil texture and short-term hydrological fluctuations (Haque et al., 2018). Natural
32 wetlands demonstrate P sink behavior compared with drained wetlands (Haque et al., 2018) and
33 the loss of small wetlands due to land conversion for agriculture or other land uses promotes P
34 loading to downstream waters. (Cheng and Basu, 2017). Intensive agriculture also influences
35 watershed hydrology and runoff patterns, generally homogenizing runoff regimes and linking
36 nutrient export and hydrological dynamics (Basu et al., 2011), although these patterns are not
37 always generalizable to snowmelt-dominated regions (Ali et al., 2017). A robust understanding
38 of the interplay between hydrological and biogeochemical controls on P mobility and transport is
39 necessary for managing landscapes to protect water quality (Sharpley et al., 1999).

40 There remain major gaps in our understanding of nutrient transport in cold, low relief
41 agricultural regions such as the Northern Great Plains. The hydrology of this region is
42 dominated by cold regions processes (Pomeroy et al., 2007); and the spring snowmelt is usually
43 the biggest hydrological event of the year, accounting for a large proportion of both annual
44 water and nutrient export (Corriveau et al., 2011; Costa et al., 2017). Historically, rates of
45 evapotranspiration in the summer coupled with low precipitation volumes have resulted in
46 relatively small contributions of growing season events to runoff in prairie streams (Shook and

47 Pomeroy, 2012). However, in the past five decades, there has been a documented increase in the
48 proportion of precipitation falling as rain and the number of multi-day summer rainstorms,
49 concurrent with a decrease in snowmelt runoff (Shook and Pomeroy, 2012; Dumanski et al.,
50 2015). Large rainfall events can result in changes to runoff pathways and dramatic nutrient
51 export, as seen in the 2014 extreme rainfall event in the Assiniboine watershed (Wilson et al., in
52 review). As winters warm and snowpacks decrease, the importance of summer hydrological
53 processes in these seasonally snow-covered regions will increase. Coupled with the ongoing
54 landuse change in this region, changes in the temperature and precipitation regimes can result in
55 dramatic changes to runoff patterns (Dumanski et al., 2015; Mahmood et al., 2017), which will in
56 turn influence P export (Wilson et al., in review). Thus, understanding how controls on nutrient
57 transport vary seasonally is critical for predicting future changes to P dynamics in this region.

58 A typical method for investigating hydrological controls on chemical behavior in watersheds is
59 via inspection of concentration-discharge (c-Q) relationships (Basu et al., 2010, 2011; Ali et al.,
60 2017). However, recent studies in this region have demonstrated that these models often have a
61 poor fit in many prairie watersheds, particularly those with steep slopes, ineffective natural
62 drainage and/or anthropogenic drainage modification (Ali et al., 2017). This may be due to the
63 high level of spatial and temporal heterogeneity in landscape sources of P and runoff (Corriveau
64 et al., 2013; Wilson et al., 2016). In many regions, intensive agriculture is associated with
65 invariant P concentrations across runoff conditions, due to large legacy stores of the nutrient
66 from years of fertilization (Basu et al., 2010; Sharpley et al., 2013). However, in contrast with
67 other regions, work from the Northern Great Plains suggests that seasonal patterns of P
68 concentrations can exhibit much more variability compared with patterns of runoff, both among
69 catchments and from year-to-year (Rattan et al., 2017). Recent work from Ali et al., (2017)

70 suggests that on the Canadian Prairies, fill and spill runoff generation during wet years and
71 seasonal changes to soil infiltration during dry years leads to variable sources of P being
72 mobilized across the landscape and thus non-chemostatic behavior. Furthermore, the spatial
73 organization of agricultural development may influence both the magnitude (Yates et al., 2014)
74 and timing (Rattan et al., 2017) of stream P concentrations. This combination of threshold-driven
75 hydrological behavior, heterogeneous spatial patterns of P sources on the landscape and extreme
76 seasonality result in complex and dynamic controls on stream P concentrations.

77 The objective of our study was to examine temporal and spatial patterns P concentrations in
78 streams in watersheds on the Northern Great Plains. Specifically, we used sub-weekly stream
79 chemistry samples and continuous discharge data from eight streams for three years to test the
80 hypothesis that controls on stream TP concentrations are regionally coherent and vary among
81 seasons.

82 **2.0 Methods**

83 *2.1 Study Area*

84 This study examined eight catchments located in the Assiniboine and Red River watersheds in
85 southwestern Manitoba (Figure 1). The climate in southwestern Manitoba is continental and
86 annually has a wide range in temperature, with an average daily temperature of 19.2 °C in July
87 and -16.5°C in January. Average daily temperatures are above zero between the months of April
88 and October, and these months are consistent with the open-water season observed during the
89 years of this study. The precipitation for the open-water season averages 366 mm total, while the
90 winter averages 96 mm total (climate data based on record from 1980-2010 for Brandon, MB
91 and retrieved from <http://climate.weather.gc.ca/>). These sites are located within the Aspen

92 Parkland and Lake Manitoba Plain ecoregions; in the past, the landscape was covered with
93 grasslands, deciduous forests and wetlands (Smith et al., 1998), but in the present day, the
94 majority of land is used for agriculture, and there is no significant urban development within
95 these catchments (Table 1). Soils in the study region were formed on gently undulating or kettled
96 calcareous glacial till. Two of the study catchments, LHOROD and RLNGR, encompass parts of
97 Riding Mountain National Park, and thus have significant forest cover and some intact natural
98 wetlands (Table 1).

99 *2.2 Stream Chemistry and Discharge Samples*

100 Water samples were taken as frequently as every few days to every few weeks from March to
101 November 2013-2015. The frequency of sampling varied by site, year and open-water season;
102 see Table 1 for the exact number of water samples from each site, as well as the acronym for
103 each site name. A well-mixed part of the stream was sampled using twice-rinsed polycarbonate
104 bottles. Samples were transported in a cooler frozen until analysis. A sulfuric acid/persulfate
105 digestion of samples was performed prior to colourimetric analysis to determine TP
106 concentration with the ascorbic acid method. It is worth noting that total dissolved phosphorus
107 was highly correlated with TP, and the dissolved fraction made up a high percentage of the TP
108 concentration in all samples, consistent with other work done in the region (McCullough et al.,
109 2012; Liu et al., 2013; Untereiner et al., 2015), and therefore all data analysis was done with TP
110 concentrations only. Water temperature at three sites (LHOROD, OR, RLNGR) was measured
111 at the time of sample collection using a hand held thermometer placed in stream near the middle
112 of the water column. Higher resolution temperature data was also collected at 2 sites (WCE,
113 WCW) with pressure transducers (Onset HOBO U20-001-04) placed on the stream bottom. For
114 six of eight streams studied sampling locations were at Water Survey of Canada (WSC)

115 hydrometric monitoring sites so discharge data was obtained from the WSC hydrometric
116 database (www.wsc.ec.gc.ca). For two sites (Willow Creek East and Willow Creek West)
117 discharge was calculated based on stage rating curves developed over three years using flow
118 measurements collected with a hand held velocity meter and half hourly depth measurements by
119 a pressure transducer (Onset HOBO U20-001-04). Resulting rating curves had a high level of
120 accuracy ($r^2 > 0.98$ at each site). More detailed methods on the calculation of streamflow at these
121 two sites are included in Wilson et al. (in review)

122 *2.3 Characterization of watersheds*

123 Soil characteristics (% sand and % clay at the 0-15 cm depths) in each watershed were quantified
124 using the 90m resolution Gridded Soil Landscapes of Canada data product from the Canadian
125 Soil Information Service (Macdonald and Kloosterman, 1984) that has been generated in support
126 of the GlobalSoilMap initiative. Land cover (% forest, % wetland and % annual cropland)
127 within each watershed was classified based on the 2006 edition of Land Use / Land Cover
128 Landsat TM Maps from the Province of Manitoba Remote Sensing Centre. Effective drainage
129 area was calculated from data from the Prairie Farm Rehabilitation Administration and is
130 representative of average runoff conditions (based on a two year return period) for the Canadian
131 prairie provinces beginning in the 1970s based on surface topography, density of the natural
132 stream network, number and size of wetlands and consultation with local residents. Average
133 slope, minimum and maximum elevation were calculated from a digital elevation model (90 m
134 resolution) derived from Shuttle Radar Topography Mission (SRTM) data.

135 *2.4 Statistical Analyses*

136 Two types of models, power law models (Equation 1) and hydrograph separation models
137 (Equation 2, Equation 3), were fit to the TP-Q data for each study catchment, following Ali et al.,
138 (2017). The power law model equation was fit as:

$$139 \quad c = aQ^b \quad \text{[Equation 1]}$$

140 where c is TP concentration, Q is discharge, a is the intercept parameter and b is the slope
141 parameter; and the hydrograph separation model was fit as

$$142 \quad \text{When } Q < \text{Thres}Q: c = C_g \quad \text{[Equation 2]}$$

$$143 \quad \text{Otherwise: } c = C_g + C_r \quad \text{[Equation 3]}$$

144 where Q is discharge, $\text{Thres}Q$ is the breakpoint, c is TP concentration, C_g is the TP concentration
145 at baseflow and $C_g + C_r$ is the solute concentration when both baseflow and runoff contribute to
146 streamflow. The same model fitting process was applied to the conductivity- Q data. The residuals
147 of the best model fit of the TP- Q , as determined by the goodness of fit (r^2) were calculated as the
148 difference between the observed and modelled values. For sites where model fit was poor
149 ($r^2 < 0.2$), residuals were calculated from a horizontal line with a y value of the mean
150 concentration. Hydrograph separation models were fit using the segmented package (Muggeo,
151 2015) to identify $\text{Thres}Q$, and the lm function to fit Equation 2 and Equation 3. In order to
152 determine if the c - Q relationships were driven by seasonal differences, the data were divided by
153 season, using visual inspection of the hydrograph to identify the end of the spring melt period,
154 and the model fitting exercise was repeated using just the spring data and just the summer data.
155 The day of year for each of the three study years was normalized to start on the first day of the
156 spring melt for each catchment, indicated by when discharge started increasing in the spring,

157 termed Days Since Melt (DSM). The catchment-specific residuals of the TP-Q models were then
158 modelled against DSM, using three types of models: a linear model, a segmented regression
159 model with one breakpoint and a segmented regression model with two breakpoints. Segmented
160 regression models were fit using the segmented package (Muggeo, 2015). Briefly, the
161 breakpoints were estimated using a bootstrap restarting algorithm which identifies local optima
162 where the linear relation changes (Wood, 2001). Goodness of fit (r^2) was calculated for all three
163 models at a significance level of $\alpha=0.05$; r^2 values exceeding 0.2, 0.4, 0.6, and 0.8 were
164 interpreted as fair, reasonable, good, and very good model fits, respectively (Ali et al., 2017).

165 For sites with significant breakpoint models, the data were divided into three time periods:
166 Period 1 (from the onset of melt to first breakpoint); Period 2 (from the first breakpoint to the
167 second breakpoint); and Period 3 (from the second breakpoint to the end of the record).

168 Catchment-specific linear regression models between the residuals of the conductivity-discharge
169 relationship and DSM, as well as stream temperature and DSM were fit for each of the three
170 periods. All statistical analyses were performed in R (R Core Team, 2017).

171 **3.0 Results**

172 *3.1 Seasonal patterns of phosphorus and discharge*

173 Discharge in the study streams followed a predictable seasonal pattern with a peak in the spring
174 associated with the spring snowmelt and a period of low flow during the summer and fall,
175 interrupted by peaks associated with rainstorms (Figure 2a). There was considerable interannual
176 variability in the magnitude and timing of storm peaks; in particular, a major storm event
177 occurred in early summer 2014, which in several streams resulted in more discharge than the
178 preceding spring melt (Wilson et al., in review). There was also a strong seasonal pattern in total

179 phosphorus (TP) concentrations across the eight study streams, with the highest concentrations
180 observed at the onset of spring melt and one or more peaks observed during the summer and fall
181 (Figure 2b). There was considerable variation among sites in the median and range of TP
182 concentrations; the predominantly forested sites (RLNGR and LHOROD) had relatively low TP
183 concentrations, while the sites dominated by annual cropland (BOYR, LASER, LASEC, OR,
184 WCE, WCW) had relatively high TP concentrations.

185 *3.2 Concentration-discharge relationships*

186 The goodness of fit (r^2) of models predicting TP from discharge ranged from not significant to
187 0.47. Of the eight sites, the power law model produced the best fit at two sites (WCW and
188 WCE), the hydrograph separation model produced the best fit at two site (BOYR and LASEC)
189 and no model producing a fair model fit ($r^2 > 0.2$) could be fit to the other four sites (Table 2;
190 Figure 3). The results were consistent when considering only the summer season, with the power
191 law producing the best fit at WCW and WCE, the hydrograph separation model producing the
192 best fit at BOYR and LASEC and the other four sites remaining with no fair model fit (Table 2).
193 Using only the spring data resulted in somewhat different patterns of model fit. Two streams
194 (LHOROD and RLNGR) had reasonable, negative relationships between TP and discharge using
195 the power law model, while LASER, LASEC and WCW had reasonable, positive relationships
196 using the power law model (Table 2).

197 *3.3 Temporal patterns and drivers of stream phosphorus*

198 Significant segmented regression models were fit between the normalized Days Since Melt
199 (DSM) and the residuals of the TP-discharge relationship at all sites except for BOYR and
200 LASEC, the two sites with the hydrograph separation TP-discharge models (Figure 4). For the

201 remaining sites, there were two significant breakpoints, which were remarkably synchronous in
202 time (breakpoint 1 ranging from day 35 to 43; breakpoint 2 ranging from day 60 to 122) (Table
203 3). These breakpoints also correspond with temporal patterns in conductivity and stream
204 temperature (Table 4). During the first period (i.e. before the first breakpoint), the residuals of
205 the conductivity-discharge relationship increased significantly from the onset of melt to the first
206 breakpoint at three sites (OR, WCE and WCW). After the first breakpoint, the patterns in
207 conductivity residuals were not coherent among sites. Temperature increased significantly
208 during the first period at three sites (LHOROD, WCE and WCW), and decreased significantly
209 during the final period (i.e. after the second breakpoint) at all sites (Table 4).

210

211 **4.0 Discussion**

212 Streams across southern Manitoba exhibit a strikingly coherent seasonal pattern of P dynamics.
213 Concentrations peak with the onset of snowmelt and decline through the spring, and generally
214 rise to a second, usually smaller peak again in the summer (Figure 2b). Examining the
215 relationships between TP and discharge at individual sites revealed generally poor model fits
216 (Figure 3), consistent with other work in the Canadian Prairies demonstrating that controls on P
217 dynamics in this region that are independent of discharge (Ali et al., 2017). Indeed, the residuals
218 of the c-Q relationships were also temporally coherent across sites, with peaks in early spring
219 and mid-summer (Figure 4). Seasonal patterns of conductivity residuals and stream temperature
220 were also synchronous with TP patterns. Conductivity residuals increased from the onset of melt
221 through to the first breakpoint (Figure 5), while stream temperatures consistently were at their
222 maxima concurrent with the second breakpoint (Figure 6). Taken together, these results suggest
223 that the mechanisms controlling patterns of stream TP concentration may vary by season.

224 *4.1 Concentration-discharge relationships*

225 There were three distinct groups of catchments based on the model fits to the TP-discharge
226 relationships: at 2 catchments, hydrograph separation models produced the best fits, at 3
227 catchments, power law models produced the best fit and at the remaining 4 catchments, no
228 models produced a reasonable model fit (Figure 3). Ali et al., (2017) found that c-Q model fits
229 were poorest in watersheds with complex drainage patterns, such as higher slopes, high
230 proportion of noncontributing areas or poorly drained soils. The four catchments with no model
231 fit, LHOROD, OR, RLNGR, and LASER are lower gradient with higher proportions of existing
232 (LHOROD, OR, RLNGR) ineffective drainage and more poorly defined contributing area.
233 LHOROD, OR, and RLNGR are located on the northwestern side of the study area and have
234 large areas with depressional or “pothole” wetlands. As a result, these three catchments have the
235 highest proportion of poorly-drained wetlands of the sites used in the study. LASER is located in
236 the Red River Valley and has been extensively drained to support agriculture, but continues to
237 experience flooding / ponding issues on agricultural land during wet seasons (McCullough et al.,
238 2012). Also, LHOROD and RLNGR encompass parts of Riding Mountain National Park, leading
239 to considerable forest cover, lower rates of soil disturbance and fertilizer input, as well as the
240 lowest median and peak TP concentrations of the study sites. These two sites have the smallest
241 proportion of annual cropland, and therefore human modification of drainage is much less in
242 these catchments (Table 1). When considering only the spring data, these two sites with
243 considerable forest cover had negative c-Q relationships (Table 2), suggesting again that the
244 sources of P within these watersheds are perhaps different. Negative c-Q relationships suggest
245 source limited systems (Moatar et al., 2017), which is consistent with low P soils in forested
246 areas.

247 The hydrograph separation model, where concentrations increase with increasing discharge only
248 above a threshold flow value, suggests that runoff generation is the primary driver of solute
249 dynamics, since baseflow concentrations are relatively flat (O'Connor et al. 1976). This suggests
250 that watersheds that exhibit this relationship are likely transport-limited, as the P is only
251 mobilized in high concentrations from landscape source areas when discharge is above a given
252 threshold (Ali et al., 2017). The two catchments where hydrograph separation models produced
253 the best fit (BOYR and LASEC) are of higher slope and span the Pembina Escarpment, which
254 overlies permeable parent material. These watersheds tend to exhibit higher water yield and
255 groundwater influence that results in the presence of baseflow. The threshold at which
256 concentration increases are observed at these sites may indicate a shift from groundwater driven
257 base flow to soil water and overland flow during runoff events. As described in Ali et al., (2017)
258 those watersheds with naturally effective drainage exhibited c-Q relationships with the highest
259 predictive ability. WCE and WCW are both naturally effectively drained and were fit with the
260 power-law (linear) c-Q model because no significant c-Q threshold was observed. These two
261 catchments differ from BOYR and LASEC in that a clear indication of a threshold shift in water
262 chemistry was not observed and may indicate that surface water inputs alone are the primary
263 driver of c-Q in well drained watersheds without significant groundwater influence.

264 *4.2 Temporal patterns and drivers of stream phosphorus*

265 The seasonal pattern of TP dynamics is consistent across catchments of varying sizes and
266 landscape characteristics (Figure 2b). This is particularly evident when examining the time
267 series of residuals of the TP-Q relationship (Figure 4). Examining the residuals of the
268 concentration-discharge relationship allows us to identify patterns in the concentration data
269 independent of the effect of discharge (Renwick et al., 2018). Positive residuals indicate that the

270 TP concentrations are higher than would be predicted from the TP-Q relationship, and negative
271 residuals indicate the concentrations are lower than would be predicted. Therefore, the coherent
272 peaks in TP-Q residuals observed in the summer are indicative of a seasonal pattern of TP
273 concentrations independent of peaks driven by summer storms. The two streams where this
274 coherent pattern is not observed (BOYR and LASEC) are the two streams where a hydrograph
275 separation model best fit the TP-Q data. In these catchments, the higher TP concentrations are
276 highly correlated to increases in discharge, meaning that, as detailed above, runoff generation
277 resulting in mobilization of phosphorus from the landscape is the dominant control on stream TP
278 concentrations. However, for the other streams in this study, discharge is not the dominant
279 control on TP. The coherence of the peak dates suggests that regional scale drivers that affect
280 availability and mobility of TP may be responsible for these patterns.

281 The pattern of decreasing TP concentrations through the snowmelt period is consistent with
282 modelling work done by Costa et al. (2017) on nitrate (NO_3) dynamics through snowmelt. In
283 that paper, the authors suggest that high NO_3 concentrations in snow and surface flow, resulting
284 from nutrient rich plant residues left on the field in the fall, result in very high concentrations in
285 the initial snowmelt, but as the melt progresses and soils thaw, runoff becomes dominated by
286 throughflow, and NO_3 concentrations decrease. The same argument could be true for TP, which
287 is also known to desorb from surface soils or leach from vegetation, and residue left on fields
288 over the winter, and can be released from during freeze-thaw cycles in the late fall (Tiessen et al.,
289 2010; Liu et al., 2013; Elliott, 2013; Whitfield et al., 2019). In this study, as in others in this
290 region, the majority of TP is in the dissolved form. Erosion of particulate P is typically not a
291 major source of P export in this landscape where the topography is flat and much of the runoff
292 occurs during the spring when soils are frozen (Salvano et al., 2009; Liu et al., 2014). This

293 flowpath-switching mechanism to explain the spring TP patterns is also supported by the
294 conductivity data. Melting snow and surface runoff will have lower conductivity than water
295 passing through ion-rich deeper soil layers, and so an inverse relationship with TP would be
296 consistent with a change in flowpaths.

297 The coherent summer peaks in stream TP concentrations are not easily explained by hydrological
298 patterns or point source inputs, as has been suggested in other studies (Corriveau et al., 2013;
299 Rattan et al., 2017). However, conductivity trends differ from TP trends in the later spring and
300 summer, indicating that a flowpath-based mechanism is unlikely to explain the coherent summer
301 peaks (Figure 5). The coherence of the peak concentrations across catchments and seasons is not
302 compatible with rainfall-driven export of TP from the landscape to the stream, given the lack of
303 coherence in the timing of storms. It is notable that the TP dynamics from 2014 are coherent
304 with the other study years, given that 2014 featured an extreme rainfall-runoff event in summer,
305 resulting in high TP export (Wilson et al., in review). This suggests that the patterns observed in
306 this dataset are robust even under years with variable hydrological regimes. Other studies have
307 suggested that seasonal release from sewage lagoons results in summer peaks in stream TP
308 (Carlson et al., 2013; Rattan et al., 2017), however in the present study, the summer patterns of
309 TP are observed across a range of watersheds, most of which are sparsely populated and have
310 little or no sewage input. This summer pattern, however, is coherent with the seasonal peak in
311 stream temperature (Figure 6), with the peak in the overprediction of TP relative to Q occurring at
312 the same point in the season as the peak stream temperature. This suggests that biogeochemical
313 processes, controlled by temperature may be responsible for this regional coherence.

314 Stream temperature will control many aquatic and soil processes that result in the removal,
315 transformation and release of P within a stream (Withers and Jarvie, 2008). These processes

316 include physical and chemical mechanisms such as dissolution and desorption reactions which
317 release bound P from soil and stream sediments (Fox, 1989), and biological mechanisms
318 including the assimilation and release of P in periphyton and phytoplankton (Dodds, 2003),
319 decomposition of both allochthonous and autochthonous organic matter (Pusch et al., 1998) and
320 uptake and decay of macrophytes (Carpenter and Lodge, 1986). During summer in the study
321 streams, adjacent riparian areas and wetlands, and in catchment soils the water movement tends
322 to be slow between runoff events while biological productivity tends to be high. These
323 conditions may leading to stagnant conditions which promote anoxia, particularly in lower
324 gradient environments and could result in release of P, particularly given the geological setting
325 of the streams (Orihel et al., 2017). Recent work has demonstrated that with rising temperatures,
326 the metabolic balance of streams shifts to higher rates of respiration compared with production,
327 promoting low oxygen conditions and potentially creating favourable conditions for P release
328 from sediments (Song et al., 2018). Any of these mechanisms could be a plausible explanation
329 for why TP concentrations (independent of discharge) decline during the late summer and early
330 fall. Given the strong association between the observed patterns in TP and stream temperature,
331 future work in this region should examine the possible in-stream and in-soil mechanisms behind
332 this pattern.

333 *4.3 Implications and future research directions*

334 Like many regions across North America, the Northern Great Plains is experiencing declining
335 snowpacks, earlier snowmelts, longer growing seasons and changes in precipitation patterns
336 during the growing season (Shook and Pomeroy 2012). The frequency, intensity and length of
337 growing season rainfall have all increased in the last several decades (Shook and Pomeroy, 2012;
338 Szeto et al., 2015; Dumanski et al., 2015). Hydrological processes and pathways of runoff

339 associated with summer rainfall in this region are fundamentally different from those which
340 predominate during spring snowmelt. For instance, surface depressional storage may regulate
341 runoff during spring melt, but if a large summer rainfall event occurs on saturated soils, the
342 surface storage may be at capacity and thus not predictive of runoff volume or pathways (Wilson
343 et al., in review). This study documents consistent seasonal patterns of high stream TP
344 concentrations during the growing season. Combined with the changes to precipitation and
345 runoff patterns, these results suggest an increasing need for management strategies which
346 account for growing season dynamics in order to mitigate excess TP export across the Northern
347 Great Plains.

348 **5.0 Conclusions**

349 Understanding the controls on P mobility and transport in agricultural landscapes is critical for
350 informing management decisions to protect water quality. There has been widespread interest in
351 understanding snowmelt dynamics, as this is the dominant hydrological event of the year in
352 northern regions, and often transports the majority of nutrients (Costa et al., 2017). Recent
353 studies have acknowledged that controls on P loading from landscapes vary seasonally
354 (Corriveau et al., 2011; Rattan et al., 2017). The results of this study suggest that controls on
355 stream P concentrations are not consistent among seasons, and that there are regionally
356 consistent patterns in stream P independent of hydrological controls. While spring P dynamics
357 are well-correlated with discharge and flowpath metrics, growing season P concentrations exhibit
358 coherent seasonal peaks across years and catchments, independent of flow dynamics. Cold,
359 agricultural regions, including the Northern Great Plains, are getting warmer, with smaller
360 snowpacks and longer summer droughts where streams are hydrologically disconnected from the
361 watershed (Schindler and Donahue, 2006). Investigating growing season stream P dynamics in

362 this landscape is critical for understanding the full picture of P cycling in these regions and for
363 making informed decisions about water quality management.

364

365 **References**

- 366 Ali, G., H. Wilson, J. Elliott, A. Penner, A. Haque, C. Ross, and M. Rabie. 2017. Phosphorus
367 export dynamics and hydrobiogeochemical controls across gradients of scale, topography
368 and human impact. *Hydrol. Process.* 31(18): 3130–3145. doi: 10.1002/hyp.11258.
- 369 Basu, N.B., G. Destouni, J.W. Jawitz, S.E. Thompson, N. V. Loukinova, A. Darracq, S. Zanardo,
370 M. Yaeger, M. Sivapalan, A. Rinaldo, and P.S.C. Rao. 2010. Nutrient loads exported from
371 managed catchments reveal emergent biogeochemical stationarity. *Geophys. Res. Lett.*
372 37(23): 1–5. doi: 10.1029/2010GL045168.
- 373 Basu, N.B., S.E. Thompson, and P.S.C. Rao. 2011. Hydrologic and biogeochemical functioning
374 of intensively managed catchments: A synthesis of top-down analyses. *Water Resour. Res.*
375 47(10): 1–12. doi: 10.1029/2011WR010800.
- 376 Bennett, E.M., S.R. Carpenter, and N.F. Caraco. 2012. Human Impact on Erodable Phosphorus
377 and Eutrophication : A Global Perspective. 51(3): 227–234.
- 378 Carlson, J.C., J.C. Anderson, J.E. Low, P. Cardinal, S.D. MacKenzie, S.A. Beattie, J.K. Challis,
379 R.J. Bennett, S.S. Meronek, R.P.A. Wilks, W.M. Buhay, C.S. Wong, and M.L. Hanson.
380 2013. Presence and hazards of nutrients and emerging organic micropollutants from sewage
381 lagoon discharges into Dead Horse Creek, Manitoba, Canada. *Sci. Total Environ.* 445–446:
382 64–78. doi: 10.1016/J.SCITOTENV.2012.11.100.
- 383 Carpenter, S.R., N.F. Caraco, D.L. Correll, R.W. Howarth, A.N. Sharpley, and V.H. Smith.
384 1998. Nonpoint Pollution of Surface Waters with Phosphorus and Nitrogen. *Ecol. Appl.*
385 8(3): 559. doi: 10.2307/2641247.

- 386 Carpenter, S.R., and D.M. Lodge. 1986. Effects of submerged macrophytes on ecosystem
387 processes. *Aquat. Bot.* 26: 341–370.
388 <http://citeseerx.ist.psu.edu/viewdoc/download?doi=10.1.1.455.3829&rep=rep1&type=pdf>
389 (accessed 26 April 2018).
- 390 Cheng, F.Y., and N.B. Basu. 2017. Biogeochemical hotspots: Role of small water bodies in
391 landscape nutrient processing. *Water Resour. Res.* 53(6): 5038–5056. doi:
392 10.1002/2016WR020102.
- 393 Corriveau, J., P.A. Chambers, and J.M. Culp. 2013. Seasonal Variation in Nutrient Export Along
394 Streams in the Northern Great Plains. *Water, Air, Soil Pollut.* 224(7): 1594. doi:
395 10.1007/s11270-013-1594-1.
- 396 Corriveau, J., P.A. Chambers, A.G. Yates, and J.M. Culp. 2011. Snowmelt and its role in the
397 hydrologic and nutrient budgets of prairie streams. *Water Sci. Technol.* 64(8): 1590–1596.
398 doi: 10.2166/wst.2011.676.
- 399 Costa, D., J. Roste, J. Pomeroy, H. Baulch, J. Elliott, H. Wheeler, and C. Westbrook. 2017. A
400 modelling framework to simulate field-scale nitrate release and transport during snowmelt:
401 the WINTRA model. *Hydrol. Process.* (August): 1–19. doi: 10.1002/hyp.11346.
- 402 Dodds, W.K. 2003. The role of periphyton in phosphorus retention in shallow freshwater aquatic
403 systems. *J. Phycol.* 39(5): 840–849. doi: 10.1046/j.1529-8817.2003.02081.x.
- 404 Dumanski, S., J.W. Pomeroy, and C.J. Westbrook. 2015. Hydrological regime changes in a
405 Canadian Prairie basin. *Hydrol. Process.* 29(18): 3893–3904. doi: 10.1002/hyp.10567.
- 406 Elliott, J. 2013. Evaluating the potential contribution of vegetation as a nutrient source in

- 407 snowmelt runoff. *Can. J. Soil Sci.* 93(4): 435–443. doi: 10.4141/cjss2012-050.
- 408 Fox, L.E. 1989. A model for inorganic control of phosphate concentrations in river waters.
409 *Geochim. Cosmochim. Acta* 53(2): 417–428. doi: 10.1016/0016-7037(89)90393-1.
- 410 Haque, A., G. Ali, M. Macrae, P. Badiou, and D. Lobb. 2018. Hydroclimatic influences and
411 physiographic controls on phosphorus dynamics in prairie pothole wetlands. *Sci. Total*
412 *Environ.* 645: 1410–1424. doi: 10.1016/J.SCITOTENV.2018.07.170.
- 413 Liu, K., J.A. Elliott, D.A. Lobb, D.N. Flaten, and J. Yarotski. 2013. Critical Factors Affecting
414 Field-Scale Losses of Nitrogen and Phosphorus in Spring Snowmelt Runoff in the Canadian
415 Prairies. *J. Environ. Qual.* 42(2): 484. doi: 10.2134/jeq2012.0385.
- 416 Liu, K., J.A. Elliott, D.A. Lobb, D.N. Flaten, and J. Yarotski. 2014. Conversion of Conservation
417 Tillage to Rotational Tillage to Reduce Phosphorus Losses during Snowmelt Runoff in the
418 Canadian Prairies. *J. Environ. Qual.* 43(5): 1679. doi: 10.2134/jeq2013.09.0365.
- 419 Macdonald, K.B., and B. Kloosterman. 1984. The Canadian Soil Information Systems (CanSIS)
420 LRRRI Contribution No. B3-59-E. Ottawa, ON.
- 421 Mahmood, T.H., J.W. Pomeroy, H.S. Wheeler, and H.M. Baulch. 2017. Hydrological responses
422 to climatic variability in a cold agricultural region. *Hydrol. Process.* 31(4): 854–870. doi:
423 10.1002/hyp.11064.
- 424 McCullough, G.K., S.J. Page, R.H. Hesslein, M.P. Stainton, H.J. Kling, A.G. Salki, and D.G.
425 Barber. 2012. Hydrological forcing of a recent trophic surge in Lake Winnipeg. *J. Great*
426 *Lakes Res.* 38(SUPPL. 3): 95–105. doi: 10.1016/j.jglr.2011.12.012.
- 427 Moatar, F., B.W. Abbott, C. Minaudo, F. Curie, and G. Pinay. 2017. Elemental properties,

- 428 hydrology, and biology interact to shape concentration-discharge curves for carbon,
429 nutrients, sediment, and major ions. *Water Resour. Res.* 53(2): 1270–1287. doi:
430 10.1002/2016WR019635@10.1002/(ISSN)1944-7973.CQCZ1.
- 431 Muggeo, M.V.M.R. 2015. Package ‘segmented’. *Regression Models with*
432 *Breakpoints/Changepoints Estimation Version*. [https://cran.r-](https://cran.r-project.org/web/packages/segmented/index.html)
433 [project.org/web/packages/segmented/index.html](https://cran.r-project.org/web/packages/segmented/index.html) (accessed 7 July 2018).
- 434 Orihel, D.M., H.M. Baulch, N.J. Casson, R.L. North, C.T. Parsons, D.C.M. Seckar, and J.J.
435 Venkiteswaran. 2017. Internal phosphorus loading in Canadian fresh waters: a critical
436 review and data analysis. *Can. J. Fish. Aquat. Sci.*: 1–25. doi: 10.1139/cjfas-2016-0500.
- 437 Pomeroy, J.W., D.M. Gray, T. Brown, N.R. Hedstrom, W.L. Quinton, R.J. Granger, and S.K.
438 Carey. 2007. The cold regions hydrological model: A platform for basing process
439 representation and model structure on physical evidence. p. 2650–2667. *In Hydrological*
440 *Processes*. Wiley-Blackwell.
- 441 Pusch, M., D. Fiebig, I. Brettar, H. Eisenmann, B.K. Ellis, L.A. Kaplan, M.A. Lock, M.W.
442 Naegeli, and W. Traunspurger. 1998. The role of micro-organisms in the ecological
443 connectivity of running waters. *Freshw. Biol.* 40(3): 453–495. doi: 10.1046/j.1365-
444 2427.1998.00372.x.
- 445 R Core Team. 2017. R. R Core Team. doi: 3-900051-14-3.
- 446 Rattan, K.J., J.C. Corriveau, R.B. Brua, J.M. Culp, A.G. Yates, and P.A. Chambers. 2017.
447 Quantifying seasonal variation in total phosphorus and nitrogen from prairie streams in the
448 Red River Basin, Manitoba Canada. *Sci. Total Environ.* 575: 649–659. doi:
449 10.1016/j.scitotenv.2016.09.073.

- 450 Renwick, W.H., M.J. Vanni, T.J. Fisher, and E.L. Morris. 2018. Stream Nitrogen, Phosphorus,
451 and Sediment Concentrations Show Contrasting Long-term Trends Associated with
452 Agricultural Change. *J. Environ. Qual.* 47(6): 1513. doi: 10.2134/jeq2018.04.0162.
- 453 Salvano, E., D.N. Flaten, A.N. Rousseau, and R. Quilbe. 2009. Are current phosphorus risk
454 indicators useful to predict the quality of surface waters in southern manitoba, Canada? *J.*
455 *Environ. Qual.* 38(September): 2096–2105. doi: 10.2134/jeq2008.0159.
- 456 Schindler, D.W. 2012. The dilemma of controlling cultural eutrophication of lakes. *Proc. R. Soc.*
457 *B Biol. Sci.* 279(1746): 4322–4333. doi: 10.1098/rspb.2012.1032.
- 458 Schindler, D.W., and W.F. Donahue. 2006. An impending water crisis in Canada’s western
459 prairie provinces. *Proc. Natl. Acad. Sci. U. S. A.* 103(19): 7210–6. doi:
460 10.1073/pnas.0601568103.
- 461 Schindler, D.W., R.E. Hecky, and G.K. McCullough. 2012. The rapid eutrophication of Lake
462 Winnipeg: Greening under global change. *J. Great Lakes Res.* 38: 6–13. doi:
463 10.1016/j.jglr.2012.04.003.
- 464 Sharpley, A.N., W.J. Gburek, G. Folmar, and H.B. Pionke. 1999. Sources of phosphorus
465 exported from an agricultural watershed in Pennsylvania. *Agric. Water Manag.* 41(2): 77–
466 89. doi: 10.1016/S0378-3774(99)00018-9.
- 467 Sharpley, A., H.P. Jarvie, A. Buda, L. May, B. Spears, and P. Kleinman. 2013. Phosphorus
468 Legacy: Overcoming the Effects of Past Management Practices to Mitigate Future Water
469 Quality Impairment. *J. Environ. Qual.* 42(5): 1308. doi: 10.2134/jeq2013.03.0098.
- 470 Shook, K., and J. Pomeroy. 2012. Changes in the hydrological character of rainfall on the

- 471 Canadian prairies. *Hydrol. Process.* 26(12): 1752–1766. doi: 10.1002/hyp.9383.
- 472 Smith, R.E., G.F. Veldhuis, R.G. Mills, R.G. Eilers, W.R. Fraser, and G.W. Lelyk. 1998.
- 473 Terrestrial ecozones, ecoregions, and ecodistricts of Manitoba: an ecological stratification
- 474 of Manitoba's natural landscapes. Technical Bulletin 98-9E.
- 475 Song, C., W.K. Dodds, J. Rüegg, A. Argerich, C.L. Baker, W.B. Bowden, M.M. Douglas, K.J.
- 476 Farrell, M.B. Flinn, E.A. Garcia, A.M. Helton, T.K. Harms, S. Jia, J.B. Jones, L.E. Koenig,
- 477 J.S. Kominoski, W.H. McDowell, D. McMaster, S.P. Parker, A.D. Rosemond, C.M.
- 478 Ruffing, K.R. Sheehan, M.T. Trentman, M.R. Whiles, W.M. Wollheim, and F. Ballantyne.
- 479 2018. Continental-scale decrease in net primary productivity in streams due to climate
- 480 warming. *Nat. Geosci.* 11(6): 415–420. doi: 10.1038/s41561-018-0125-5.
- 481 Szeto, K., J. Brimelow, P. Gysbers, and S. R. 2015. The 2014 extreme flood on the southeast
- 482 Canadian Prairies. *Bull. Am. Meteorol. Soc.* 96(12): 20–24. doi: 10.1175/BAMS-D-15-
- 483 00110.
- 484 Tiessen, K.H.D., J.A. Elliott, J. Yarotski, D.A. Lobb, D.N. Flaten, and N.E. Glozier. 2010.
- 485 Conventional and Conservation Tillage: Influence on Seasonal Runoff, Sediment, and
- 486 Nutrient Losses in the Canadian Prairies. *J. Environ. Qual.* 39(3): 964. doi:
- 487 10.2134/jeq2009.0219.
- 488 Untereiner, E., G. Ali, and T. Stadnyk. 2015. Spatiotemporal variability of water quality and
- 489 stable water isotopes in intensively managed prairie watersheds. *Hydrol. Process.* 29(18):
- 490 4125–4143. doi: 10.1002/hyp.10579.
- 491 Whitfield, C.J., N.J. Casson, R.L. North, J.J. Venkiteswaran, O. Ahmed, J. Leathers, K.J.
- 492 Nugent, T. Prentice, and H.M. Baulch. 2019. The effect of freeze-thaw cycles on

- 493 phosphorus release from riparian macrophytes in cold regions. *Can. Water Resour. J. / Rev.*
494 *Can. des ressources hydriques*: 1–14. doi: 10.1080/07011784.2018.1558115.
- 495 Wilson, H.F., N.J. Casson, A.J. Glenn, P. Badiou, and L. Boychuk. In review. Landscape
496 controls on nutrient export during snowmelt and an extreme rainfall runoff event in northern
497 agricultural watersheds. *J. Environ. Qual.* MS# JEQ-2018-07-0278-AWG
- 498 Wilson, H.F., S. Satchithanatham, A.P. Moulin, and A.J. Glenn. 2016. Soil phosphorus spatial
499 variability due to landform, tillage, and input management: A case study of small
500 watersheds in southwestern Manitoba. *Geoderma* 280: 14–21. doi:
501 10.1016/j.geoderma.2016.06.009.
- 502 Withers, P.J.A., and H.P. Jarvie. 2008. Delivery and cycling of phosphorus in rivers: A review.
503 *Sci. Total Environ.* 400(1–3): 379–395. doi: 10.1016/J.SCITOTENV.2008.08.002.
- 504 Wood, S.N. 2001. Minimizing Model Fitting Objectives That Contain Spurious Local Minima by
505 Bootstrap Restarting. *Biometrics* 57(1): 240–244. doi: 10.1111/j.0006-341X.2001.00240.x.
- 506 Yates, A.G., R.B. Brua, J. Corriveau, J.M. Culp, and P.A. Chambers. 2014. Seasonally driven
507 variation in spatial relationships between agricultural land use and in-stream nutrient
508 concentrations. *River Res. Appl.* 30(4): 476–493. doi: 10.1002/rra.2646.
- 509
- 510

511 List of Figures

512 Fig. 1. Eight sub-catchment study sites in southwestern Manitoba. Data obtained from
513 Agriculture and Agri-food Canada.

514 Fig 2. Seasonal patterns of a) discharge and b) total phosphorus concentration in eight streams
515 for three years. The x axis is standardized such that day zero is the day of peak discharge during
516 the spring melt period.

517 Fig 3. Relationships between total phosphorus concentration and discharge at eight streams in
518 southern Manitoba. Data were collected in three years (2013, 2014, 2015). Solid black lines
519 indicate significant model fits. Solid grey lines indicate mean concentrations where no
520 reasonable model fit was possible.

521 Fig 4. Time series of the residuals of the total phosphorus-discharge relationship. Solid lines
522 indicate significant piece-wise regression models. Vertical lines indicate the breakpoints
523 identified in that model

524 Fig. 5 Time series of the residuals of the conductivity-discharge relationship. The vertical lines
525 are breakpoints identified from the TP time series analysis.

526 Fig. 6 Time series of water temperature. The vertical lines are breakpoints identified from the
527 TP time series analysis.

528

Table 1. Site characteristics. Numbers in each year refer to the total number of total phosphorus samples collected.

Site Name	Site Acronym	2013	2014	2015	Effective Drainage Area (%)	Wetland (%)	Annual Cropland (%)	Forest (%)	Sand (%)	Clay (%)	Minimum elevation (masl)	Maximum elevation (masl)	Average slope (%)
Roseisle Creek	BOYR	34	34	24	90.59	0.80	70.53	12.8	2.82	0.27	302	514	2.18
Little Saskatchewan near Horod	LHOROD	39	43	14	65.84	13.44	5.14	55.6	8.47	0.00	558	725	1.96
La Salle River near Elie	LASER	54	85	20	100.00	0.08	83.10	2.73	0.02	80.4	237	265	0.69
Elm Creek Channel	LASEC	27	27	19	49.78	0.18	40.03	25.1	36.45	34.6	244	306	0.99
Oak River	OR	16	70	62	23.65	10.42	57.71	5.29	0.38	0.00	459	679	1.15
Rolling River new Erickson	RLNGR	31	43	15	88.78	11.03	8.51	56.6	3.99	5.56	550	755	2.78
Willow Creek East Branch	WCE	89	112	59	98.43	1.69	74.97	1.93	0.00	1.58	376	474	1.27
Willow Creek West Branch	WCW	92	126	71	65.41	3.52	72.82	3.98	0.00	3.88	377	474	1.08

Table 2: Fits of models predicting total phosphorus concentration from discharge. The power law model is described in Equation 1 and the hydrograph separation model is described in Equations 2 and 3. ThresQ is the breakpoint ln-transformed discharge. NA indicates that no breakpoint could be located using the model fitting algorithm, and therefore no model could be fit.

Power law model		Hydrograph separation model			
All seasons					
Site	p value	r ²	p value	r ²	ThresQ
BOYR	<0.01	0.08	<0.01	0.34	-0.36
LASER	0.04	0.03	0.01	0.05	-2.20
LASEC	<0.01	0.34	<0.01	0.46	-1.05
LHOROD	0.32		0.27		
OR	0.12		0.06		
RLNGR	0.83		0.35		
WCE	<0.01	0.33	<0.01	0.14	0.38
WCW	<0.01	0.47	<0.01	0.30	-0.61
Spring					
Site	p value	r ²	p value	r ²	ThresQ
BOYR	0.32		0.07		
LASER	<0.01	0.32	NA		
LASEC	<0.01	0.55	0.02		
LHOROD	<0.01	0.30	0.72		
OR	0.35		0.15		
RLNGR	0.02	0.25	0.05		
WCE	0.44		0.31		
WCW	<0.01	0.36	NA		
Summer					
Site	p value	r ²	p value	r ²	ThresQ
BOYR	0.17		<0.01	0.23	-0.36
LASER	0.01	0.05	<0.01	0.09	-2.18
LASEC	<0.01	0.23	<0.01	0.35	-4.73
LHOROD	0.96		0.91		
OR	0.08		0.16		
RLNGR	0.29		0.10		
WCE	<0.01	0.23	0.22		
WCW	<0.01	0.48	<0.01	0.32	-0.79

Table 3: Fits of models predicting the residuals of the total phosphorus-concentration model from Days Since Melt.

Site	Linear regression model		Segmented model (one breakpoint (BP))			Segmented model (two breakpoints (BP))			
	p value	r ²	p value	r ²	BP 1 (Days Since Melt)	p value	r ²	BP 1(Days Since Melt)	BP 2 (Days Since Melt)
BOYR	0.55		0.11			0.07			
LASER	0.01	0.04	<0.01	0.13	105.86	<0.01	0.46	40.75	58.09
LASEC	0.60		0.59			0.11			
LHOROD	0.35		<0.01	0.23	27.10	<0.01	0.32	43.17	86.05
OR	0.30		0.05			<0.01	0.56	37.09	122.33
RLNGR	0.03	0.05	0.02	0.17	36.36	<0.01	0.38	43.09	70.50
WCE	<0.01	0.05	<0.01	0.26	26.03	<0.01	0.48	35.32	78.13
WCW	0.02	0.02	<0.01	0.33	27.63	<0.01	0.49	36.12	90.96

Table 4: Linear regression relationships between days since melt and residuals of the conductivity-discharge relationship and water temperature, respectively.

	Site	Conductivity			Water temperature		
		p value	r ²	slope	p value	r ²	slope
Period 1 Onset of melt to first breakpoint	LASER	0.35					
	LHOROD	0.72			0.00	0.38	8.15
	OR	0.04	0.12	0.01	0.27		
	RLNGR	0.06			0.11		
	WCE	0.00	0.24	0.01	0.00	0.93	12.39
	WCW	0.00	0.32	0.02	0.03	0.73	9.88
Period 2 1st breakpoint to 2nd breakpoint	LASER	0.01	0.20	0.02			
	LHOROD	0.10			0.00	0.43	46.37
	OR	0.00	0.22	0.02	0.32		
	RLNGR	0.55			0.91		
	WCE	0.67			0.07		
	WCW	0.24			0.01	0.70	64.76
Period 3 2nd breakpoint to end of record	LASER	0.09					
	LHOROD	0.95			0.00	0.34	-32.59
	OR	0.00	0.19	-0.02	0.01	0.83	-27.40
	RLNGR	0.40			0.00	0.41	-45.72
	WCE	0.00	0.07	0.02	0.00	0.80	-68.79
	WCW	0.01	0.06	-0.03	0.01	0.68	-46.50

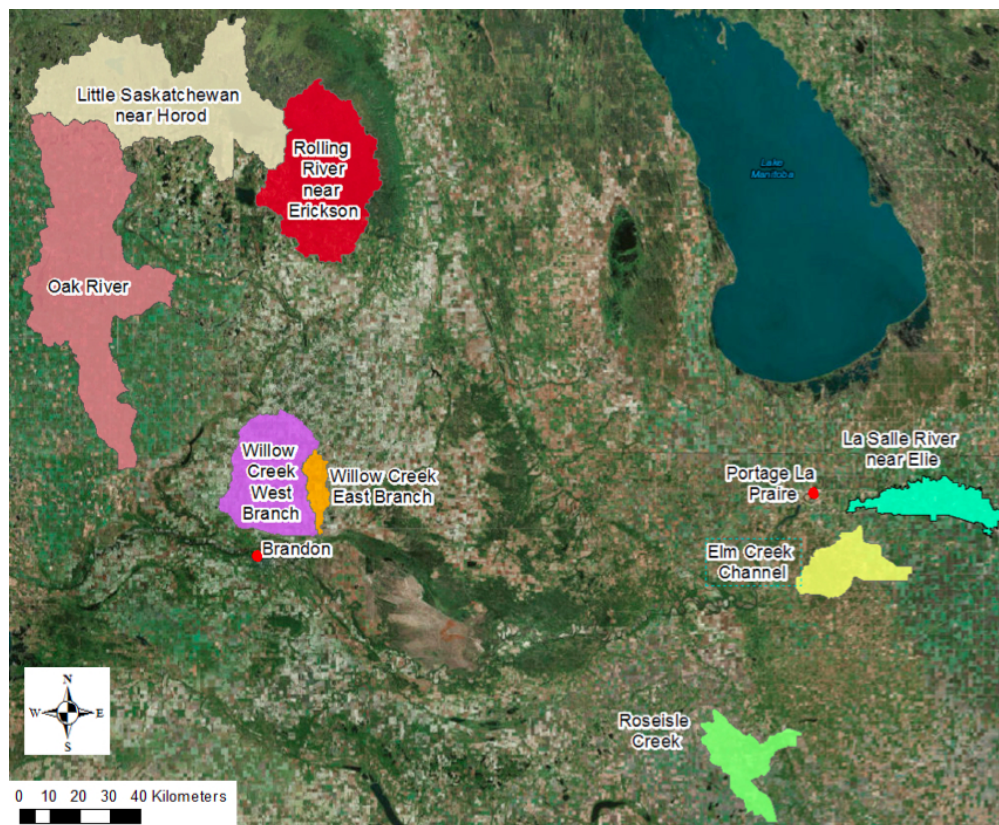


Fig. 1. Eight sub-catchment study sites in southwestern Manitoba. Data obtained from Agriculture and Agri-food Canada.

300x247mm (72 x 72 DPI)

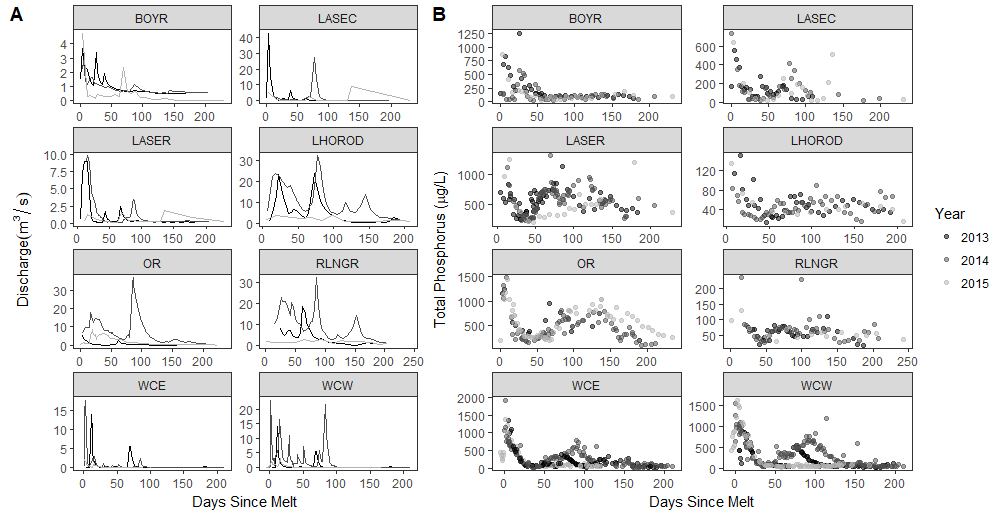


Fig 2. Seasonal patterns of a) discharge and b) total phosphorus concentration in eight streams for three years. The x axis is standardized such that day zero is the day of peak discharge during the spring melt period.

264x137mm (96 x 96 DPI)

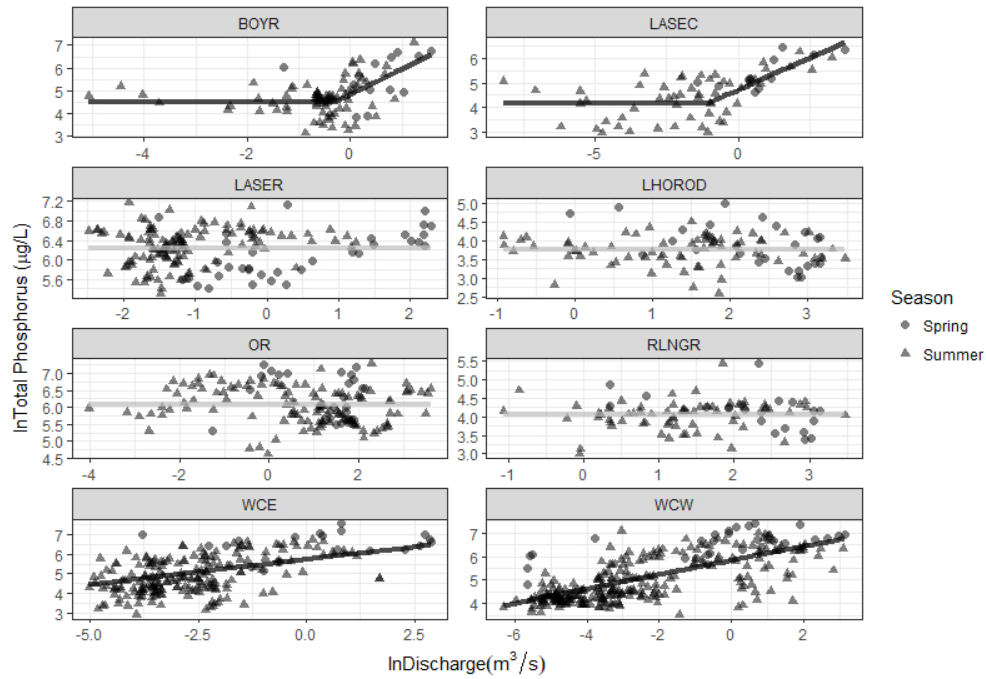


Fig 3. Relationships between total phosphorus concentration and discharge at eight streams in southern Manitoba. Data were collected in three years (2013, 2014, 2015). Solid black lines indicate significant model fits. Solid grey lines indicate mean concentrations where no reasonable model fit was possible.

211x146mm (96 x 96 DPI)

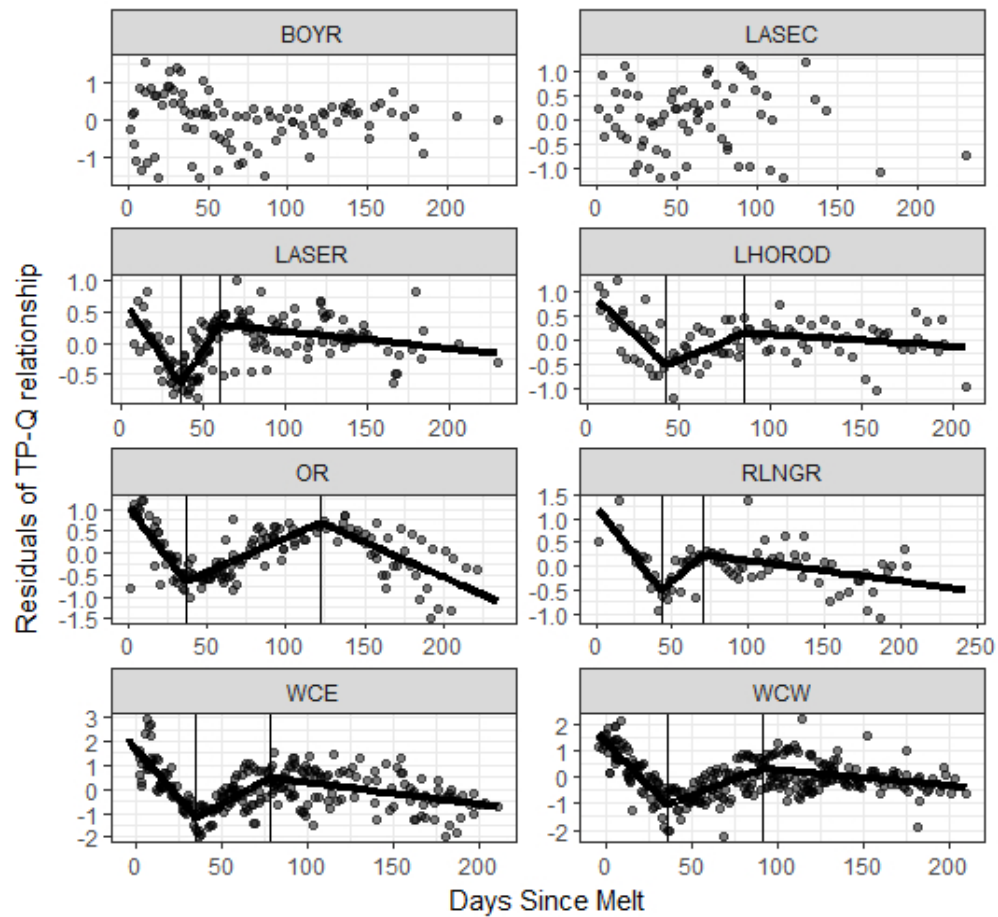


Fig 4. Time series of the residuals of the total phosphorus-discharge relationship. Solid lines indicate significant piece-wise regression models. Vertical lines indicate the breakpoints identified in the model.

141x132mm (96 x 96 DPI)

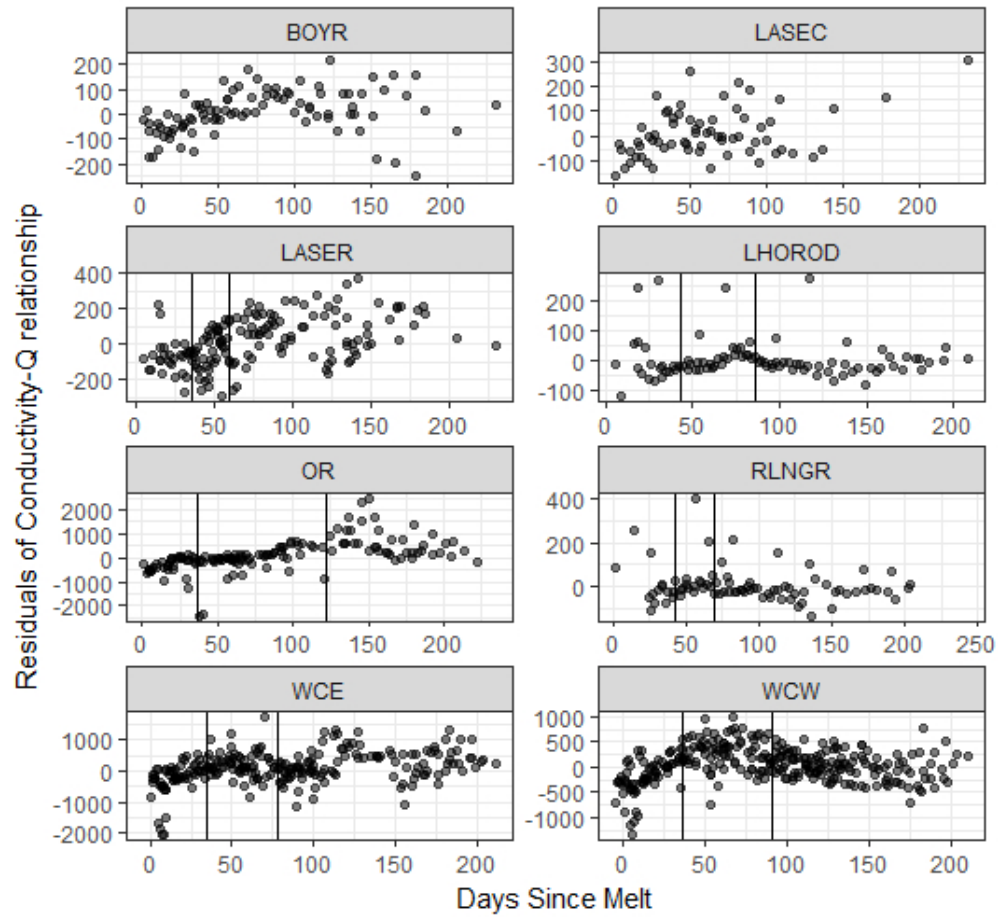


Fig. 5 Time series of the residuals of the conductivity-discharge relationship. The vertical lines are breakpoints identified from the TP time series analysis.

141x132mm (96 x 96 DPI)

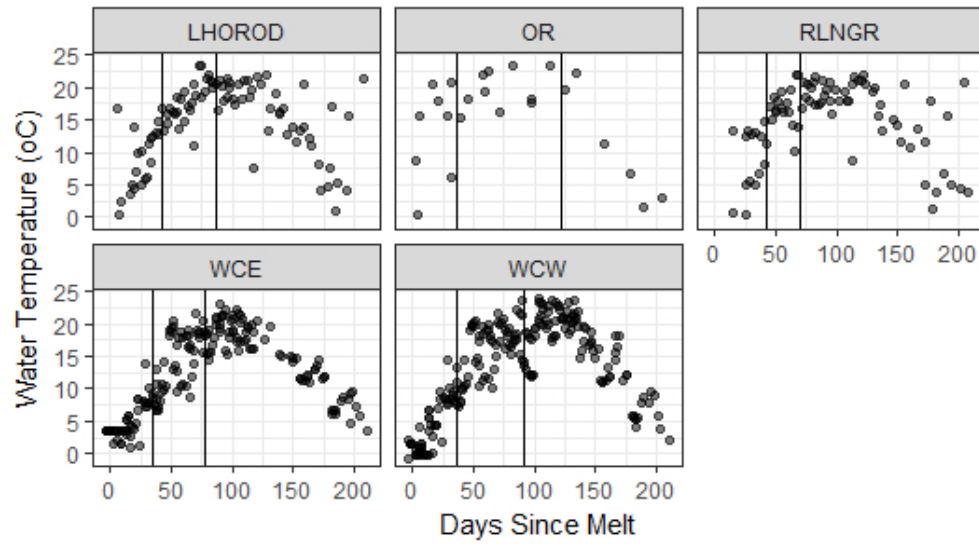


Fig. 6 Time series of water temperature. The vertical lines are breakpoints identified from the TP time series analysis.

141x79mm (96 x 96 DPI)